Arch. Metall. Mater. **71** (2026), 2, 425-430

DOI: https://doi.org/10.24425/amm.2026.158821

NURIN AISYAH AHMAD OMAR[1], ADZRIE BAHARUDIN[1], ROZYANTY RAHMAN[2], SOLHAN YAHYA[1], ZULIAHANI AHMAD[1*], WAN IZHAN NAWAWI WAN ISMAIL[1]

MECHANICAL AND CONDUCTIVE PROPERTIES OF SILICONE FILLED GRAPHENE ELECTRICALLY CONDUCTIVE ADHESIVE (ECA)

Electrically conductive adhesives (ECAs) are promising alternatives to traditional solders for flexible and lightweight electronic packaging. However, achieving high conductivity while maintaining good mechanical flexibility remains challenging. This study aims to develop a silicone-based graphene ECA modified with polyethylene glycol (PEG-600) to improve electrical and mechanical performance. Silicone/graphene ECAs were fabricated with varying graphene contents (0-9 wt.%) through controlled sonication and curing. The samples were characterized using tensile testing, Fourier Transform Infrared Spectroscopy (FTIR), Scanning Electron Microscopy (SEM), and Electrochemical Impedance Spectroscopy (EIS). FTIR spectra confirmed successful graphene incorporation through the presence of –OH, CH, C=C, and C=O functional groups, with the –OH peak shifting to higher intensity at 7% loading. Electrical conductivity reached an optimum of 4.87×10^{-6} S/cm at 9% graphene, attributed to the formation of continuous electron pathways within the polymer matrix. Mechanical tests revealed maximum tensile strength (0.305 MPa) and Young's modulus (146.523 MPa) at 7% graphene before decreasing due to filler agglomeration. SEM analysis supported these findings with uniform filler dispersion at optimum loading. The synergistic addition of graphene and PEG-600 effectively enhanced conductivity and mechanical stiffness, demonstrating strong potential for flexible electronic applications.

Keyword: Electrical conductive adhesives; electrical impedance spectroscopy; silicone; graphene

1. Introduction

The electronic packaging industry has traditionally utilized the soldering technique, namely lead-based solders, to establish electron paths and interconnect electronic components [1]. Soldering with lead uses a high temperature, about 150°C along with high current and voltage usage also can produce dust and fumes which are hazardous and can cause respiratory problem when inhaled [2]. Lead has the potential to produce water and soil pollution, which can subsequently have adverse effects on organisms and the environment. Exposure to high levels of lead can result in the development of anemia, damage to the kidneys and brain, and disruption of the reproductive and developmental systems [3]. Therefore, Electrical Conductive Adhesives (ECA) has a great potential for substituting the conventional soldering technique.

ECA is a type of glue that can conduct electricity, generally used in electronics. It consists of different polymers such as silicone, epoxy, polyurethane, or polyamide and conductive fillers such as carbon-based, ceramic, metal, or metal-coated fillers. It is commonly employed in microelectronic assemblies to establish reliable mechanical, electrical and thermal interconnections of electronic lightweight. Silicone adhesives have good electrical properties and can be modified to function as insulators with high dielectric strength, which explain why it has a long history of usage for electronics. But silicone was known as electrical insulation components [3]. ECA has the advantages of controlled viscosity, high line resolution, wide range of sample adaptation, and low temperature interconnection and recognizable benefits such as being harmless to the ecosystem, low soldering temperature, higher adaptability, good economy value, and the ability of microscale designing [4]. It can be made using a blend of conductive filler and polymer. There is a lot of polymers widely used for ECA such as epoxy, polyamide, and silicone that offers lead-free solder alternatives for component attachment on various range of applications.

Silicone materials (organosiloxanes) are high-value polymers with immense stability and durability against UV light and high temperature, chemical inertness, weather resistance, and characteristics. Thus, introducing a conductive filler to the polymer matrix can help in solving this problem. Various fillers,

[1] UNIVERSITI TEKNOLOGI MARA (UITM) PERLIS BRANCH, FACULTY OF APPLIED SCIENCES, 02600 ARAU, PERLIS, MALAYSIA
[2] UNIVERSITI MALAYSIA PERLIS (UNIMAP), CENTRE OF EXCELLENCE GEOPOLYMER AND GREEN TECHNOLOGY (CEGEOGTECH), PERLIS, MALAYSIA
* Corresponding author: zuliahani@uitm.edu.my

including silver, gold, carbon black, nickel, carbon nanotubes, and graphene, have been used to enhance the conductivity of the ECAs [5]. Among all, GR gives many advantages such as high electron mobility at room temperature, high thermal conductivity, improved mechanical strength, exhibit room temperature quantum Hall effect, and high optical transparency [6,7]. Graphene is a layer of carbon particles, which pack in a honeycomb crystal lattice cross-section in a two-dimensional design [6]. There are different strategies used to create conductive graphene in huge scope with high conductivity and minimal expense such as electrochemical intercalation, Hummer's method, and liquid sonication method.

Contrast to that, liquid sonication is a safe and easy to use method that can produced high quality graphene composite. The ultrasonication method is used with different loading percentages of filler (0%, 3%, 5%, 7%, and 9%) as its manipulated variables. Percentage of graphene affects the dispersion of graphene as well as defining the molecular scale forces and aggregation which will influence the final properties of graphene. Graphene content was found to be affecting its morphology – The higher the graphene percentage in a composite, the easier it will agglomerate, causing damages to its structure. Optimum amount of graphene can significantly increase tensile strength, decrease flexural strength and nanocomposites [8]. Polyethylene glycol (PEG), a non-ionic amphiphilic polymer, serves as an effective surfactant and compatibilizer [9]. PEG facilitates improved interfacial adhesion and enhances graphene dispersion, resulting in the creation of more homogeneous and functional PDMS/graphene nanocomposites [10]. The synergy among these materials opens new possibilities for high-performance composites in flexible electronics, sensors, and biomedical applications.

Thus, in continuation for the search of potential materials to replace hazardous solder- lead method. This work was focused on the utilization of silicone filled GR ECA under the influence of various GR loading with PEG via ultrasonication method on its mechanical and electrical characteristics.

2. Experiment

The materials used in this study include silicone-based poly(dimethylsiloxane) (PDMS), graphene nanoplatelets, polyethylene glycol (PEG-600), and Sylgard-184 curing agent. PDMS serves as the primary binder, characterized by a density of 965 kg/m^3 and a molecular weight of approximately 100,000. Graphene nanoplatelets, with a molecular weight of 12.01, are employed as conductive particles to enhance the composite's electrical properties. Polyethylene glycol (PEG-600), possessing a density of 1.13 g/cm^3 at 20°C, is utilized as a surface modifier to improve the dispersion and interfacial compatibility between the hydrophobic PDMS and the graphene filler. Sylgard-184 was used as a curing agent, featuring a specific gravity of 1.03 kg/m^3 at 25°C, to initiate the crosslinking process during the curing of the PDMS matrix.

Graphene nanoplatelet samples with varying concentrations (0%, 3%, 5%, 7%, and 9%) were mixed with distilled water and subjected to sonication for 30 minutes at room temperature using a power of 960 W and a vibration frequency of 20 kHz. The purpose of this process was to enhance the dispersibility of the graphene nanoplatelets. The silicone (PDMS) was combined with PEG-600 and immersed in a water bath for a duration of 2 hours at a temperature of 75°C. Subsequently, it was agitated using a magnetic stirrer for an additional 2 hours at a speed of 600 revolutions per minute, while maintaining a temperature of 80°C. Subsequently, the GNP/distilled water suspension was introduced into the PDMS-PEG mixture and subjected to agitation for a duration of 4 hours at a temperature of 120°C and a speed of 600 rpm, with the objective of eliminating the distilled water. Afterwards, hardener was progressively added to the samples and casted on glass moulds plate with a dimension of 1 cm × 2 cm × 0.2 cm (width × length × thickness) underwent a curing procedure in an oven at a temperature of 100°C for a period of 4 hours. Once dried, the ECAs were stored in a sealed container before being tested.

Fourier Transform Infrared Spectroscopy (FTIR)

The FT-IR spectrum of the materials was acquired by means of Thermo Electron Corporation Nicholet 380 over a range of 400-4000 cm^{-1} with a resolution of 4 cm^{-1} using KBr pressed pellet technique. A homogenous mixture was prepared by combining the powdered sample with KBr in a 1: 10 ratios. The mixture was then pressing to produce transparent disc.

Electrochemical Impedance Spectroscopy (EIS)

The EIS was performed by using the Autolab Potentiostat following Hazirah et al., (2022), and the results were evaluated using the Nova 1.11 software. 10^3 to 10^6 hertz were set for the testing frequency, and 0.3 volts was the amplitude that was applied [11]. The film samples specimen was cut into 1 cm^2 of area for this testing. The results of the conductivity test were acquired from the data. The graph was analyzed so that the electrical conductivity can be determined. The following equation used to determine the conductivity value, which is denoted by σ. The calculation for conductivity is;

$$\sigma = t/R_b A$$

Where;

σ – electric conductivity (S/cm^{-1}),
t – thickness of film (cm),
R_b – bulk resistance,
A – area of electrode.

Tensile testing (ASTM D412 Shore A)

Tensile tests were conducted according to the ASTM D412 Shore A standard. These tests comprised subjecting a sample specimen to a tensile force and assessing several features of the specimen while it was under stress. The trials were carried out

using an Instron 3382 universal tensile machine. The loading rate was adjusted to 500 mm/min using the dumbbell shape fabricated with the ASTM D412 C-type, shore A tensile standard, with dimensions of 3.2 mm thickness, 115 mm length, 6 mm width, and a gauge length of 33 mm.

3. Results and discussion

Mechanical properties of the ECA

Fig. 1 showed the effect of percentage loading of graphene nanoplatelet on the tensile properties of PDMS-PEG ECAs filled graphene nanoplatelet. It can be seen that the tensile strength of PDMS-PEG ECA filled with graphene nanoplatelet increased drastically at percentage loading of 5% at 0.327 MPa, then decreases at 7% and 9% percentage loading at 0.305 Mpa and 0.174 MPa, respectively. The GNP loading of 0% and 3% show the lowest value, indicating that the presence of GNP effectively increased the tensile strength of the adhesive composite. It is believed at 3% GNP, the utilization of GNP in PDMS is not sufficient enough to give strength to the composite system. The GNP 3% composite have the same value as the composite with no GNP can be due to the low concentration of GNP in the composite. Previous studies stated that, the tensile strength of a composite increases with the increasing percentage of graphene content until it reached a maximum (optimum) loading percentage [11]. Excessive loading percentage of GNP can cause the tensile strength of composite to deteriorate, which can be seen in GNP 7% and 9%. In addition, the utilization of GNP in nanosize provide high aspect ratio for enhanced surface interaction between the constituent's materials [12].

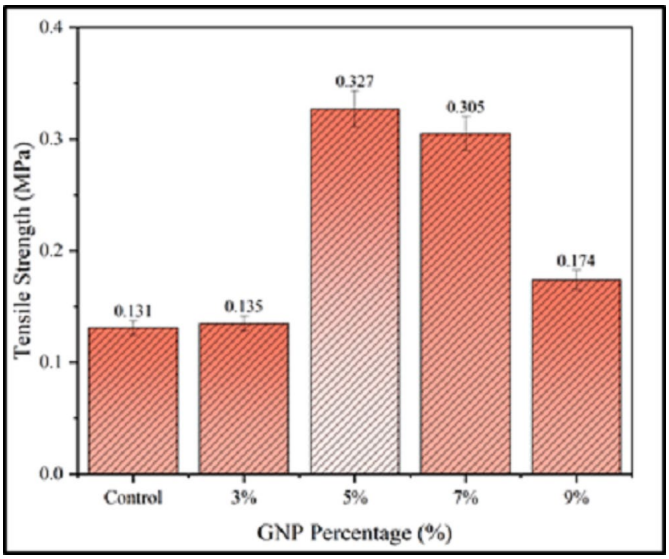

Fig. 1. Tensile strength against GNP percentage loading of PDMS-PEG filled graphene conductive adhesive (cured mould)

The impact of graphene nanoplatelet loading on the Young's modulus for PDMS-PEG ECA filled graphene is depicted in Fig. 2. The Young's modulus exhibits a similar pattern to the tensile strength results as an increment as GNP loading percent in the conductive adhesive increases until it reaches saturation. Indicating that too much GNP content in the composite ultimately caused the mechanical strength of the composite to drop, the value declined at 9% of GNP loading with a strength of 106.583 MPa. The optimum value is at 7% GNP loading with a value of 146.523 MPa, followed by 9% GNP at 106.5083 MPa, 5% GNP at 76.144, 3% GNP at 15.723 MPa, and 0% GNP at 0.054 MPa. This indicates that a composite's stiffness may be significantly increased by including GNP.

As mentioned in the section above, the strong interfacial contact between the GNPs and the matrix and the excellent dispersion of GNPs in the matrix enhances the stress transfer from the PDMS-PEG matrix to the GNP at low contents (5% and 7%), improving stiffness and strength. It can be seen that the addition of graphene regardless of the increased of strength is due to the inherent stiffness of graphene [13]. The presence of GNP clusters at 9% would cause the stress to concentrate, readily causing fracture formation to limit the efficiency of stress transmission between the matrix and the GNP, lessening the reinforcing effect [14]. Therefore, it can be claimed that GNP has the optimum loading content in the composite at 7%.

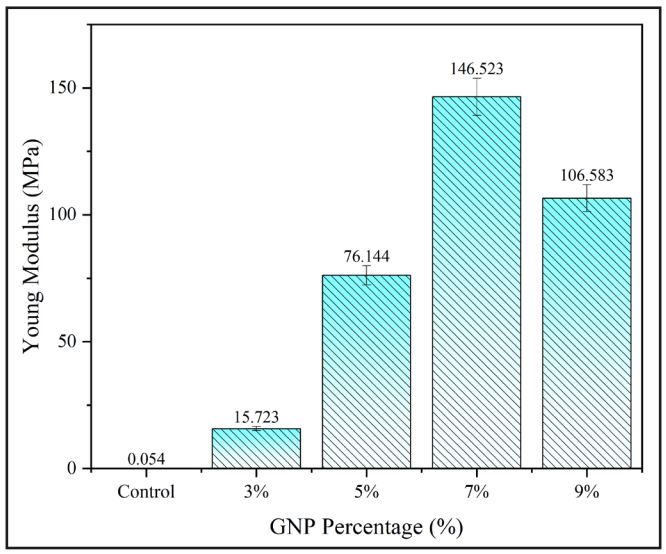

Fig. 2. Young's modulus against GNP percentage loading of PDMS-PEG filled graphene conductive adhesive

Conductivity study

In order to fully comprehend the electrical characteristics of electrochemical materials, such as the impedance of conductive film, the complex impedance spectrum (Nyquist plots/Cole-Cole plot) approach was a well-known and potent instrument. Silicone rubber naturally has a high level of insulation where has an intrinsic resistivity of around 1014 Ω/cm [2]. However, the conductivity of the insulating rubber matrix further rises when conductive filler is combined with graphene nanoplatelets. The impedance behaviour of PDMS-PEG filled graphene nanoplate-

lets in the frequency range of 5 kHz to 4 MHz where has two regions: a spike in the high-frequency zone and a semicircle toward the lower frequency region. The linear zone dominates the plots for GNP with 0% loading and GNP with 9% loading, indicating that a diffusion-limited mechanism has a significant effect on the electron transfer that takes place on the electrode surface [15]. The Warburg impedance (Zw), which indicates that the impedance is a resultant of the diffusion layer between the bulk solution and the electrode surface, is a common representation of the diffusion-limited process [16,17]. It only comprises of a semicircle at the low frequency area for GNP 3%, 5%, and 7%, indicating that the Warburg impedance has little of an impact on the PDMS-PEG ECA filled GNP. As a result of the presence of GNP at the electrode interface, the data further imply that the electrode exhibits a somewhat capacitive characteristic.

0% GNP sample is a reference from previous study that also used silicone ECA with a value of conductivity of 7.06×10^{-09} S/cm [11]. The reason why control sample from previous study was used is due to the control sample prepared in this study showed a high conductivity value (the obtained conductivity was 1.33×10^{-07} S/cm), which may be caused by errors during sample preparation and defects on the composite, hindering the samples to perform higher electrical abilities. According to the TABLE 1, the adhesive's conductivity gradually increases up to 7% GNP then went up as high as up to 4.87×10^{-07} S/cm at 9% GNP, having the highest conductivity among the samples. Utilization of enhanced graphene in ECA improves the conductivity regardless the percentage. This is due to the graphene inherent properties of electrical conductivity [18]. This demonstrates how the addition of GNP may improve a composite's conductivity. The adhesive lasts longer when the sample has a high conductivity because the electrolytes will be drawn to the composite and oxidized there rather than seeping into the substrate.

TABLE 1

GNP loading and conductivity value

GNP loading (%)	Conductivity (S/cm)
0	7.06×10^{-09}
3	1.42×10^{-08}
5	1.58×10^{-08}
7	2.52×10^{-07}
9	4.87×10^{-07}

Characterization of *FTIR* analysis

In Fig. 3 above, the FTIR spectra of PDMS/PEG-600 (0%) and PDMS/PEG-600/GNP (3,5,7 and 9%) were displayed. The spectra were captured at ambient temperature in the range of 4000-600 cm^{-1}. Testing revealed that the spectra display bands with the stretching and bending vibration of the samples. The –OH stretch group from PEG-600 may be seen in the IR spectra of PDMS/PEG-600 at absorption band 3453.44 cm^{-1}. At 2961.64 cm^{-1} and 2876.27 cm^{-1}, the stretching bands of the –CH2 group in PDMS and the –OH group from PEG-600 are both present. Adsorption band for the functional group –CH3 at 1257.76 cm^{-1} belongs to PDMS. For the Si–O–C, Si–O–Si, and Si–C groups, respectively, adsorption at 1066.52 cm^{-1}, 1016.67 cm^{-1}, and 692.28 cm^{-1} belongs to PDMS [11]. The reported FTIR spectra also show the existence of GNP in the matrix. As can be observed, the broad band centered at 3442.03 cm^{-1} represents the hydroxyl groups (O–H), and that might be a result of the hydroxyls on the surface of GNPs [19]. At 2873.73 cm^{-1} and 2920 cm^{-1}, the bands correspond to the CH group's stretching vibrations could be seen. The skeletal vibration's C=C stretching is responsible for the absorption peak at 1645.72 cm^{-1}, which

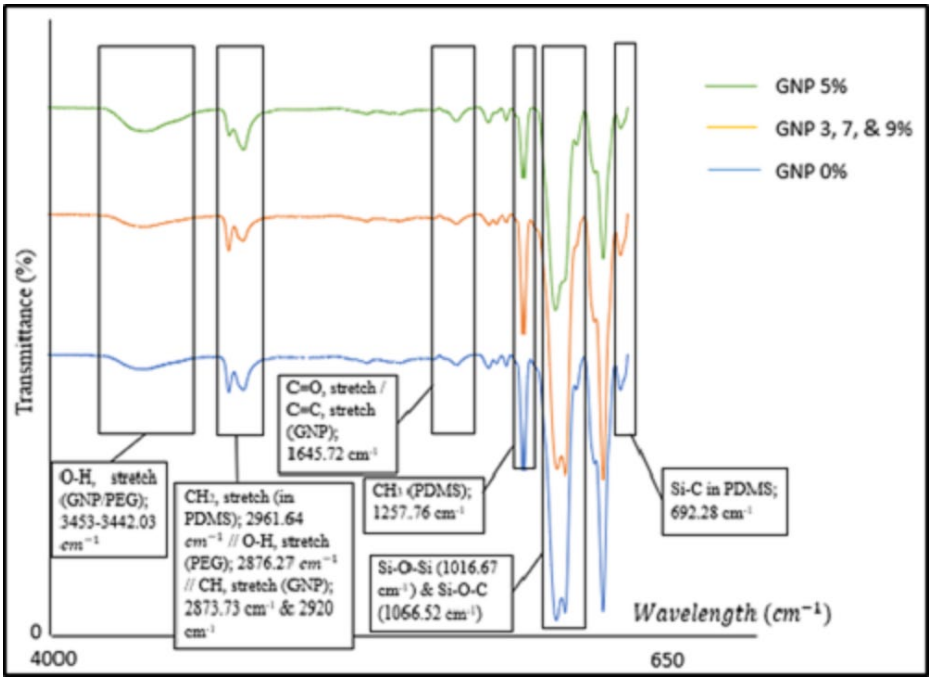

Fig. 3. FTIR spectroscopy for PDMS-PEG ECA

may also be a band of the C=O adsorption group. The FTIR spectra are similar for all percentage loadings of GNP (3%, 7%, and 9%), with the exception of the depth intensity of the –OH stretching band at 3440 cm^{-1}, which has been shifted due to different concentration of GNPs [11]. As seen in the figure, the largest –OH band belongs to the GNP 5%.

Characterization of *Scanning Electron Microscopy* (SEM)

The SEM analysis reveals distinct morphological differences between the control silicone rubber and the graphene-reinforced composite. In the control sample, the surface appears smooth and uniform, indicating a homogenous silicone rubber matrix with no visible presence of conductive fillers or structural irregularities. This morphology is typical of pure silicone rubber, where the absence of reinforcement results in a relatively featureless surface under high magnification. In contrast, the graphene-incorporated sample (ECA 7%) shows a significantly rougher and more heterogeneous surface. The microstructure is populated with irregular, flaky features suggestive of dispersed graphene or carbon black particles. These structures confirm the successful integration of the conductive filler into the silicone matrix. The distribution of graphene appears reasonably widespread, although certain regions display signs of particle agglomeration [20]. Such agglomeration may influence the consistency of the composite's electrical and mechanical performance [21]. Overall, the morphological changes observed in the SEM image of the composite confirm that the inclusion of graphene alters the internal structure of silicone rubber.

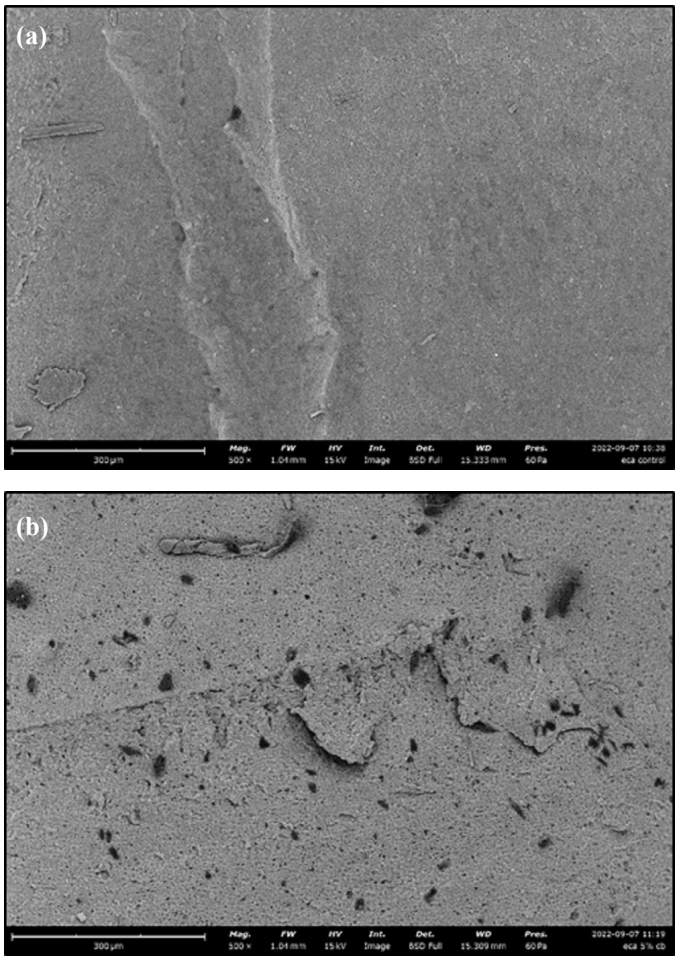

Fig. 4. SEM imaging for (a)control and (b)7% GNP for 500×

4. Conclusions

In general, this research project was successfully studied, leading to several important advances to our understanding about conductive adhesive as a whole. The optimum loading percentage for the PDMS-PEG ECA in this experiment is found at 7% GNP content. This is because the amount of GNP in the conductive adhesive was high enough to allow it to diffuse easily into the PDMS-PEG resin, improving both its mechanical and conductive qualities [22]. After the GNP had been loaded to its maximum potential, the research was proceeded by monitoring it in a variety of tests, including conductivity, FTIR, and tensile. The experiment demonstrated that adding more GNP to a composite material improved its mechanical capabilities, but further adding more GNP would cause those properties to degrade. The chain mobility of silicone-filled GNP is reduced when the surface contact of the material increases [6]. Increase of GNP content will also result in increment of stiffness. It is found that at 7% loading GNP sample shows an optimum tensile strength (0.305 MPa) and Young's modulus (146.523 MPa). To improve the conductivity qualities, the adhesive composite can also be treated with an ionic salt or a silane coupling agent that can increased the utilization of the filler which can be extend with the plastic waste containing conductive filler [23].

Acknowledgments

This work was supported by Universiti Teknologi MARA (UiTM), Malaysia. The author would like to thank Faculty of Applied Sciences (FSG), ARAUCAT Laboratory, UiTM Perlis for providing the facilities and laboratory materials used in this research project and also Centre of Excellence Geopolymer and Green Technology (CEGeoGTech), Universiti Malaysia Perlis (UniMAP), Perlis, Malaysia.

REFERENCES

[1] X. Zhang, Preparation of silver nanopowders and its application in low temperature electrically conductive adhesive. Microelectron. Reliab. 142, October, 114917 (2023).
DOI: https://doi.org/ 10.1016/j.microrel.2023.114917

[2] Z.S. Hamrah, V.A. Lashgari, M.H.D. Mohammadi, D. Uner, M. Pourabdoli, Microstructure, resistivity, and shear strength of electrically conductive adhesives made of silver-coated copper powder. Microelectron. Reliab. **127**, 9, 114400 (2021).
DOI: https://doi.org/ 10.1016/j.microrel.2021.114400

[3] M.H. Azhar et al., Electrical and Mechanical Properties of Silicone Electrically Conductive Adhesive (ECAs) Filled Graphene-Carbon Black. Sci. Lett. **19**, 1, 1-12 (2025).

[4] L.T. Tseng, R.H. Jhang, J.Q. Ho, C.H. Chen, Molecular Approach to Enhance Thermal Conductivity in Electrically Conductive Adhesives. ACS Applied Electronic Materials **1** (9), 1890-1898 (2019). DOI: https://doi.org/10.1021/acsaelm.9b00401

[5] K. Chen, Investigation of graphene-based multi-filler Electrically conductive adhesive material [Master's thesis, University of Akron]. (2019).

[6] N. Koosha, J. Karimi-Sabet, M.A. Moosavian, Y. Amini, Improvement of synthesized graphene structure through various solvent liquids at low temperatures by chemical vapor deposition method. Materials Science and Engineering: B **274**, 115458 (2021). DOI: https://doi.org/10.1016/j.mseb.2021.115458

[7] Z. Zhen, H. Zhu, Structure and Properties of Graphene. Graphene 1–12 (2018).
DOI: https://doi.org/10.1016/b978-0-12-812651-6.00001-x

[8] G. Seretis, I. Theodorakopoulos, D. Manolakos, C. Provatidis, Effect of sonication on the mechanical response of graphene nanoplatelets/glass fabric/epoxy laminated nanocomposites. Composites Part B: Engineering **147**, 33-41 (2018).
DOI: https://doi.org/10.1016/j.compositesb.2018.04.034

[9] P.K. Karoki, S. Zhang, C.M. Cai, P.E. Dim, A.J. Ragauskas, Thermally stable and self-healable lignin-based polyester. Polym. Test. **137**, June, 108515 (2024).
DOI: https://doi.org/10.1016/j.polymertesting.2024.108515

[10] D. Yan, Z. Chen, W. Zhang, Y. Wang, L. Chen, Multifunctional anti-corrosion coatings based on 2D/3D structure-function integrated nanomaterials for steel protection. Prog. Org. Coatings **206**, 4, 109335 (2025).
DOI: https://doi.org/10.1016/j.porgcoat.2025.109335

[11] H.N. Hazirah, A. Zuliahani, M.N. Sarip, A. Faiza, A.S. Samsudin, Y.D. Arief, Electrical and Mechanical Properties of Silicone Electrical Conductive Adhesives (ECAs) Filled Carbon Black Treated with 3-Aminotriethoxysilane at Elevated Temperature. Int. J. Integr. Eng. **14**, 3, 63-69 (2022).
DOI: https://doi.org/ 10.30880/ijie.2022.14.03.007

[12] J. Zhan, Z. Lei, Y. Zhang, Non-covalent interactions of graphene surface: Mechanisms and applications. Chem. **8** (4), 947–979 (2022). DOI: https://doi.org/10.1016/j.chempr.2021.12.015

[13] D.G. Papageorgiou, I.A. Kinloch, R.J. Young, Mechanical properties of graphene and graphene-based nanocomposites. Progress in Materials Science **90**, 75-127 (2017).
DOI: https://doi.org/10.1016/j.pmatsci.2017.07.004

[14] N.J. Huang, J. Zang, G.D. Zhang, L.Z. Guan, S.N. Li, L. Zhao, L.C. Tang, Efficient interfacial interaction for improving mechanical properties of polydimethylsiloxane nanocomposites filled with low content of graphene oxide nanoribbons. RSC Advances **7** (36), 22045-22053 (2017).
DOI: https://doi.org/10.1039/c7ra02439h

[15] K. Park, B.Y. Chang, S. Hwang, Correlation between Tafel Analysis and Electrochemical Impedance Spectroscopy by Prediction of Amperometric Response from EIS. ACS Omega **4** (21), 19307-19313 (2019).
DOI: https://doi.org/10.1021/acsomega.9b02672

[16] N. Izzati Ramli, N. Alya Batrisya Ismail, F. Abd-Wahab, W. Wardatul Amani Wan Salim, Cyclic Voltammetry and Electrical Impedance Spectroscopy of Electrodes Modified with PEDOT:PSS-Reduced Graphene Oxide Composite. Transparent Conducting Films. (2019). DOI: https://doi.org/10.5772/intechopen.80715

[17] H.S. Magar, R.Y.A. Hassan, A. Mulchandani, Electrochemical Impedance Spectroscopy (EIS): Principles, Construction, and Biosensing Applications. Sensors **21** (19), 6578 (2021).
DOI: https://doi.org/10.3390/s21196578

[18] B. Alemour, et al., Review of electrical properties of graphene conductive composites. International Journal of Nanoelectronics and Materials **11** (4), 371-398 (2018).

[19] A.J. Galante, et al., Coal-Derived Functionalized Nano-Graphene Oxide for Bleach Washable, Durable Antiviral Fabric Coatings. ACS Applied Nano Materials **5** (1), 718-728 (2022).
DOI: https://doi.org/10.1021/acsanm.1c03448

[20] W. Zhang et al., Surface treatment of micron silver flakes with coupling agents for high-performance electrically conductive adhesives. Int. Journal Adhesion Adhesive **122**, November 2022, 103300 (2023).
DOI: https://doi.org/10.1016/j.ijadhadh.2022.103300

[21] S.N. Kasa, et al., Effect of unmodified and modified nanocrystalline cellulose reinforced polylactic acid (PLA) polymer prepared by solvent casting method morphology, mechanical and thermal properties. Mater. Plast. **54** (1), 91-97 (2017).

[22] M.F.A. Hashim, et al., Effects of Different Fiber Sizes in PLA/Carbon Fiber Composites on Mechanical Properties. Archives of Metallurgy and Materials **69**, 2, 723-732 (2024).
DOI: https://doi.org/10.24425/amm.2024.149803

[23] M.A. Platon, at al., The Influence of Process Parameters on the mechanical Behavior of a Composite Material Made from Mixed Plastic Wastes. Archives of Metallurgy and Materials **67** (4), 1235-1241 (2022).
DOI: https://doi.org/10.24425/amm.2022.141047